

# Microstructural Changes of Phenolic Resin during Pyrolysis

TSE-HAO KO,<sup>1</sup> WEN-SHYONG KUO,<sup>2</sup> YING-HUANG CHANG<sup>1</sup>

<sup>1</sup> Department of Materials Science, Carbon Fibers Laboratory, Feng Chia University, Taichung, Taiwan, Republic of China

<sup>2</sup> Department of Aeronautical Engineering, Feng Chia University, Taichung, Taiwan, Republic of China

Received 18 May 2000; accepted 16 September 2000

**ABSTRACT:** After curing, phenol-formaldehyde resins were postcured at 230°C in air for 32 h and then carbonized and graphitized from 300 to 2400°C. Thermal fragmentation and condensation of the polymer structure occurred above 300°C. The crystal size of the cured phenolic resins decreased with the temperature increase. Above 600°C the original resin structures disappeared completely. Below 1000°C the stack size ( $L_c$ ) and crystal size ( $L_a$ ) were small. Above 1000°C the  $L_c$  increased with the increasing treatment temperature. The carbonized and graphitized resins were characterized using Raman spectroscopy. Below 400°C there were no carbon structures in the Raman spectra analysis. Above 500°C the G and D bands appeared. The frequency of the G band of all carbonized and graphitized samples shifted to 1600  $\text{cm}^{-1}$  from the 1582  $\text{cm}^{-1}$  of graphite. The D band shifted to 1330  $\text{cm}^{-1}$  from the 1357  $\text{cm}^{-1}$  of the imperfect carbon. The carbonized and graphitized phenolic resins could not be considered as truly glassy or amorphous carbon materials because they had some degree of order in the basal plane. However, the crystal size was very small even at 2400°C. © 2001 John Wiley & Sons, Inc. *J Appl Polym Sci* 81: 1084–1089, 2001

**Key words:** Raman spectrometry; X-ray diffraction; phenolic resin; microstructure; pyrolysis

## INTRODUCTION

The interest of the aerospace industries in carbon/carbon (C/C) composites has rapidly increased over the past decade.<sup>1–4</sup> At a high temperature these composites retain their strength, modulus, and mechanical properties while other materials do not.<sup>5,6</sup> Phenolic resins reinforced with carbon fibers can serve as starting materials for the preparation of C/C composites.<sup>7</sup> The pyrolysis of carbon/phenolic composite materials is an important step in the manufacture of C/C materials, which

are low density materials that retain excellent mechanical properties to temperatures above 2000°C. It is well known that the microstructure of the matrix during pyrolysis has a significant influence on the final mechanical properties of C/C composites. The pyrolysis reactions convert the phenolic matrix to amorphous carbon.<sup>8–10</sup> In the transition from resin to amorphous (glassy) carbon, the evolution of low molecular weight compounds and the condensation of the polymer structure take place.<sup>9–17</sup> These reactions lead to the development of shrinkage, the formation of pores, and weight loss. It can also be expected that the mechanical properties of the final carbonized resins will be dependent on the formation of the microstructures of the resin during pyrolysis. There are apparently no literature data concerning the influence of the pyrolysis process (400–2400°C) on the microstructural changes in the

---

Correspondence to: T.-H. Ko (thko@fcu.edu.tw).  
Contract grant sponsor: National Science Council; contract grant number: NSC88-2216-E-035-001.  
Contract grant sponsor: Feng Chia University; contract grant number: FCU-RD-87-01.

*Journal of Applied Polymer Science*, Vol. 81, 1084–1089 (2001)  
© 2001 John Wiley & Sons, Inc.

phenolic resin. Wide-angle X-ray diffraction and Raman spectroscopy are used to measure the microstructural changes in the material during pyrolysis.

## EXPERIMENTAL

The resol-type phenol-formaldehyde resin was supplied by Chang Chun Petrochemical Industry (Taiwan) as a 60 wt % solid content solution. The phenolic resin was concentrated under a vacuum at 70°C for 8 h and at 80°C for 8 h. It was then poured into aluminum plates and cured in an oven from 80 to 150°C for several hours. Following this, the resin was cured at 160°C for 2 h and slowly cooled (2°C/min) to room temperature. The cured resins were cut to an appropriate size (6 × 1 × 0.3 cm). The cured samples were postcured in air at 230°C for 32 h. All samples were pyrolyzed at a heating rate of 1°C/min from 300 to 1000°C in nitrogen. The graphitized resins were graphitized to 1800 and 2400°C at a rate of 15°C/min in an argon flow.

The density was measured at 25°C according to the density gradient column method. The density gradient column was prepared with a mixture of *n*-heptane and carbon tetrachloride so that a gradient of about 1.2–1.6 g/mL extended from top to bottom. For the measurement of the density range of 1.6–2.0 g/mL a density gradient column prepared with a mixture of carbon tetrachloride and 1,3-dibromopropane was adopted.

An X-ray diffractometer (model 8536, Diano) that provided Ni-filtered Cu K $\alpha$  radiation was used to measure the crystalline-related properties of the samples. The step-scan method was used to determine the *d* spacing and stacking size ( $L_c$ , stacking height of layer planes). The step interval was set at 0.02°. The *d* spacing and  $L_c$  were calculated using eqs. (1) (the Bragg equation) and (2) (the Scherrer equation), respectively:

$$n\lambda = 2d \sin \theta \quad (1)$$

$$L_c(hkl)(\text{nm}) = K\lambda/B \cos \theta \quad (2)$$

in which  $\lambda = 0.1542$  nm,  $K$  is the apparatus constant (1.0), and  $B$  is the half-value width (rad) of the X-ray diffraction intensity ( $I$ ) versus the  $2\theta$  curve.

The Raman spectrometer used here was a Renishaw 2000 instrument with a Raman imaging microscope system, which had the 514.5-nm line

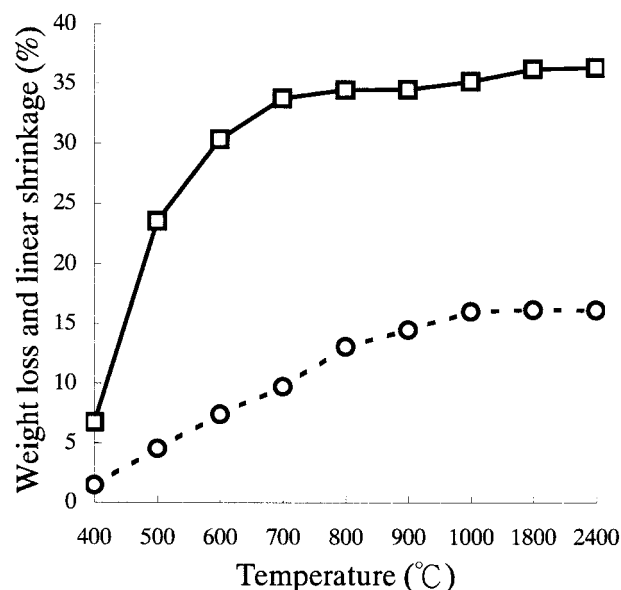


**Figure 1** The variation of the weight loss and shrinkage of resulting carbonized resins as a function of the pyrolysis temperature: (□) weight loss and (○) shrinkage.

of an argon ion laser as the incident radiation. The samples were analyzed without any treatment or preparation. The scattered light was analyzed using a double-grating monochromator and detected by a cooled photomultiplier tube.

## RESULTS AND DISCUSSION

### Changes in Weight Loss, Shrinkage, and Density

Figure 1 represents the weight loss and linear shrinkage during pyrolysis. The weight loss was determined from the change in weight between postcured and final samples. During the pyrolysis stage, noncarbon elements in the resin were removed as volatiles, such as H<sub>2</sub>O, CO, CO<sub>2</sub>, H<sub>2</sub>, and other gases.<sup>8–15</sup> These reactions were due to the condensation of aromatic ribbon moleculars in the cured resin and the volatilization of low molecular weight species. These reactions also led to the weight loss and shrinkage of the resin during pyrolysis. The weight loss was significant between 400 and 700°C, and it was nearly completed by 1800°C. The weight losses in the pyrolysis temperature ranges of 400–700, 700–900, 900–1800, and 1800–2400°C were about 27.1, 0.7, 1.8, and 0.1%, respectively. The amount of evolved gases in the heat-treatment temperature range of 400–700°C was more than 90% of that evolved during pyrolysis. At this stage the con-

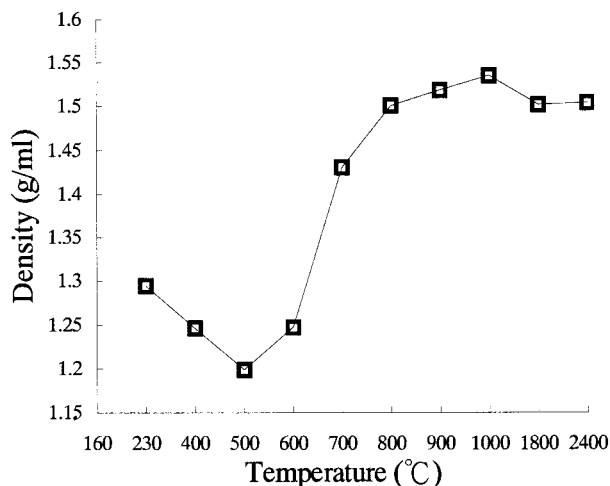


**Figure 2** The variation of the density of resulting carbonized resins as a function of the pyrolysis temperature.

condensation reactions and the crosslink reactions occurred in the cured resin. The polymeric structures of the cured resin were slowly transferred into the glassy carbon.

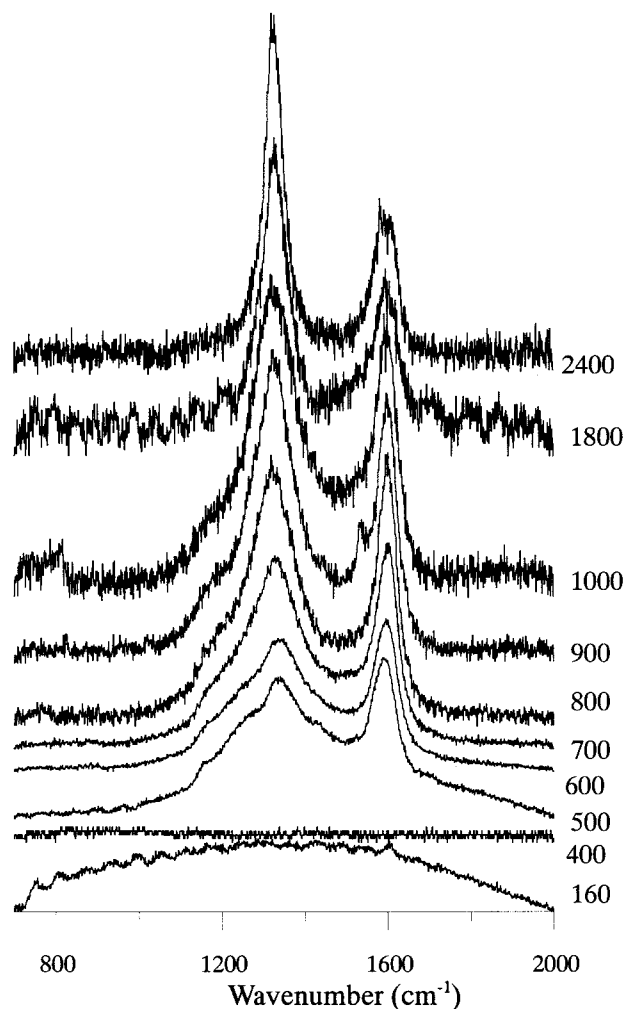
Compared with the behavior of the weight loss, shrinkage occurred continuously at about 1000°C, as shown in Figure 1. Below 700°C the shrinkage linearly increased with increasing temperature. This shrinkage was due to the condensation and crosslink reactions of polymeric structures to form the glassy carbon. Above 700°C the shrinkage was mainly due to the rearrangement of the carbon structure. Above 1000°C the shrinkage was very slow. This was attributable to the repacking and crosslinking of the glassy carbon structure.

Figure 2 shows the variation in the bulk density during pyrolysis. There were two factors affecting the bulk density of the heat-treated sample.<sup>11</sup> One was pore formation, and the other was chemical densification caused by the chemical structure change of the resin during pyrolysis. At the early stage of pyrolysis, because of the condensation of polymeric structures, the evolved gases created a lot of pores in the carbonized sample.<sup>18</sup> Below 700°C the weight loss and the shrinkage are relatively dominant. Therefore, the density decreases with increasing temperature and reaches a minimum value of 1.199 g/mL at 500°C. At the higher pyrolysis temperature, the polymeric structures of the resin gradually transform into the glassy carbon structure, the evolved gases may pass easily through the preexisting pores without further volume expansion, and the

effect of chemical densification is higher than the formation of new pores during pyrolysis. Therefore, at 1000°C the maximum value of 1.536 g/mL is reached. Above 1000°C the density decreases. This is due to structure rearrangement and the formation of closed pores from open pores.<sup>8,19,20</sup> The increase of the bulk density above 1800°C is considered to result from the chemical structure change, the condensation, and crosslinking of the carbon basal planes during graphitization.

### X-Ray Diffraction Observation

Structural changes during carbonization were followed by X-ray diffraction. Figure 3 shows the diffraction profiles for the phenol-formaldehyde resin during pyrolysis. The figure shows the cured resin (cured at 160°C) and the resin heat treated from 230 to 2400°C. The cured resin showed a

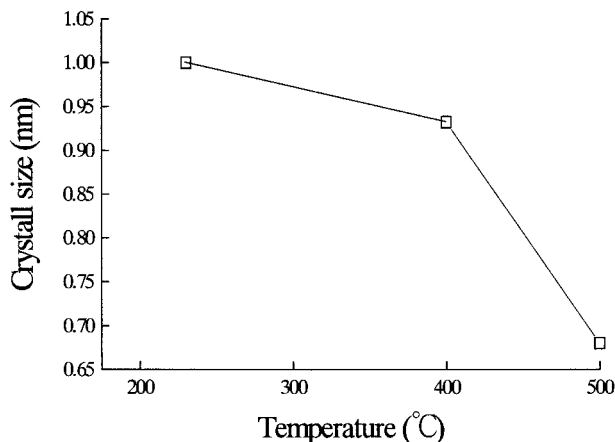


**Figure 3** The wide-angle X-ray diffraction patterns of cured resins during pyrolysis.

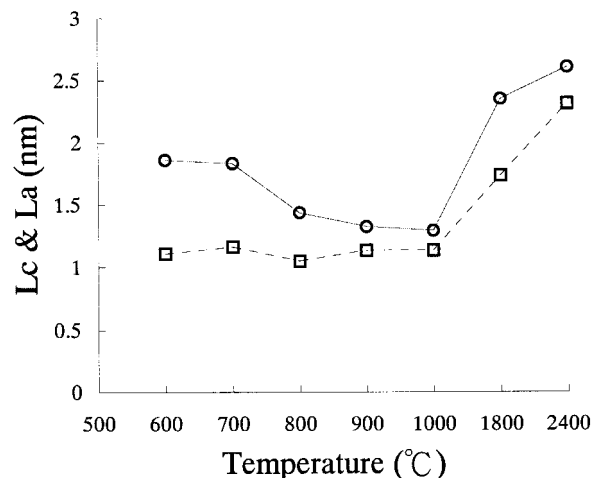
broad maximum peak at  $2\theta \approx 19^\circ$ , which was due to adjacent chains of linear polymer<sup>16</sup>; this peak became broader and less intense with the increasing heat-treatment temperature. Above 600°C this peak completely disappeared. At 500°C the new peak appeared at  $2\theta \approx 23^\circ$ . This peak shifted to around  $2\theta \approx 25^\circ$  from  $23^\circ$  when the temperature rose above 600°C. Another new peak was also found near  $2\theta \approx 43^\circ$ . This peak was due to the formation of glassy carbon structures from polymer structures. These peaks corresponded to (002) and (10) reflections of carbon materials. Diffraction profiles (002) and (10) of the glassy carbon structures were very weak at 500°C. Above 600°C the two diffraction profiles gradually increased in intensity. This was due to the lengthening and broadening of the carbon basal planes from polymeric structures.

Figure 4 represents the variation in the crystal size of the cured resin with the temperature of the heat treatment. The crystal size of the cured resins decreased from 1.00 to 0.68 nm when the heat-treatment temperature rose from 230 to 500°C. It is well known that noncarbon elements in the cured resins are removed as volatiles when the resins are heat treated above 300°C.<sup>8,13,14</sup> Thermal fragmentation and condensation of the polymer structure also occurred above 300°C. These reactions led to the decrease in crystal size of the cured resins. Finally, these structures were transferred into the glassy carbon above 500°C.

Figure 5 shows the variation in stacking size ( $L_c$ ) during pyrolysis. Below 1000°C the  $L_c$  increased very slowly. This indicated that the structure in the carbonized resin was very random and disordered. Above 1000°C the  $L_c$  increased very fast. This was due to the formation of the isotropic structures.



**Figure 4** The variation of the crystal size of cured resins as a function of the heat-treatment temperature.



**Figure 5** The variation of the stacking height ( $L_c$ ) and crystal size ( $L_a$ ) of resulting carbonized resins as a function of the pyrolysis temperature: (□) stacking height and (○) crystal size.

#### Raman Spectra Analysis

Tuinstra and Koenig<sup>21</sup> first published the first-order Raman spectrum of a graphite single crystal. This spectrum exhibited a single characteristic line at  $1575\text{ cm}^{-1}$ , which was thereafter designated the G band (for graphite). A second band at  $1360\text{ cm}^{-1}$ , which occurred with the G band in the spectra of polycrystalline graphite,<sup>21</sup> was designated the D band (for defects). The D band, which has a low intensity in graphite and well-organized materials, becomes equivalent or even more intense than the G band for more disordered solids. In addition to these two major bands, the existence of other smaller ones was further postulated, principally to improve fitting in the deconvolution of spectra. The D' band was found at  $1620\text{ cm}^{-1}$  for relatively well-ordered materials.<sup>22</sup> The D'' band was found at about  $1500\text{ cm}^{-1}$  in carbon films.<sup>23,24</sup>

Figure 6 shows the Raman spectra of cured resins during pyrolysis. The resin cured at 160°C showed a weak and broad band from 700 to 2000  $\text{cm}^{-1}$ . This corresponded to the polymeric structures of a phenolic resin. At 400°C the Raman spectra did not show any peak. This indicated that no carbon structures were formed at this temperature. Above 500°C the Raman spectra showed two strong wide bands near 1582 and 1357  $\text{cm}^{-1}$ . The peak located near 1582  $\text{cm}^{-1}$  was due to the graphitic structure whereas that near 1357  $\text{cm}^{-1}$  was due to a disordered structure in the carbon. In this study the real D and G bands were not located at 1357 and 1582  $\text{cm}^{-1}$ . The

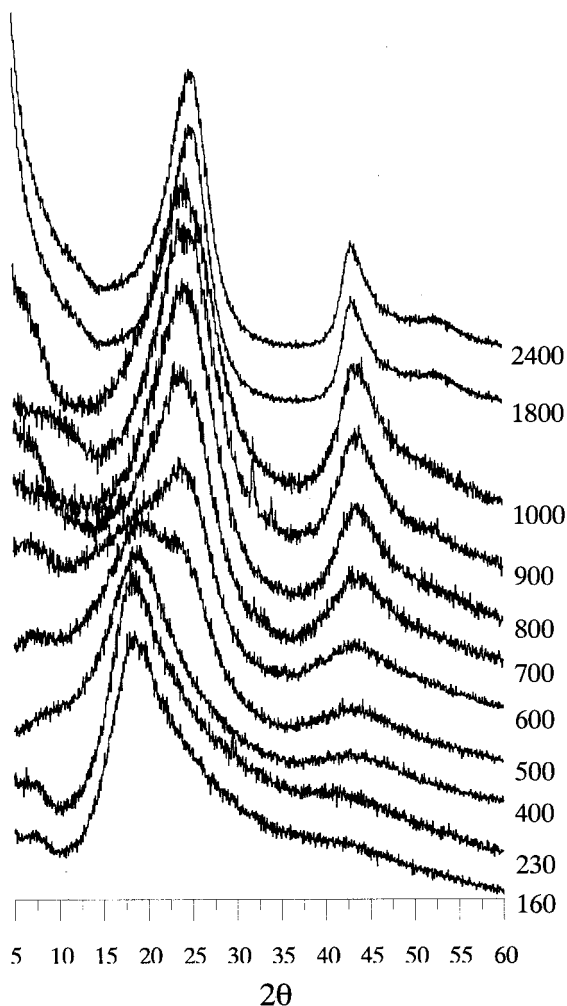


**Figure 6** Raman spectra of resulting carbonized and graphitized resins after pyrolysis.

peaks shifted to  $1330$  and  $1600\text{ cm}^{-1}$ , respectively, when the samples were heat treated above  $500^\circ\text{C}$ . Cottinet et al.<sup>25</sup> used the small size of the area analyzed in Raman microprobe spectrometry to measure the spectra from two different zones of a pitch. They found the two typical bands at  $1360$  and  $1580\text{ cm}^{-1}$  in the mesophase zone whereas only one at  $1600\text{ cm}^{-1}$  was found in the isotropic zone. They considered the band at  $1600\text{ cm}^{-1}$  for the microcrystalline order. Green et al.<sup>26</sup> found the G band at  $1600\text{ cm}^{-1}$  in the spectra of coals. In this study the bands at  $1600\text{ cm}^{-1}$  were also considered to be in the G band for the microcrystalline order, because these samples had a small crystal size ( $L_a$ ) and crystal stacking ( $L_c$ ), as shown in Figure 5.

In this study the D band shifted to  $1330\text{ cm}^{-1}$  from  $1357\text{ cm}^{-1}$ , as shown in Figure 6. Cuesta et al.<sup>27</sup> found a Gaussian band centered at about

$1330\text{ cm}^{-1}$  in the activated carbons. This Gaussian shape corresponded to a nonhomogenous defect or impurity ions. They designated this band as the I band (for impurity ions). In our study this peak was very narrow and sharp at  $2400^\circ\text{C}$ . All impurity ions evolve at this temperature. Therefore, this peak was due to a disorder not to impurity ions.

It is now generally accepted that the dependence between the integrated intensity ratio  $I(D)/I(G)$  can be calculated by the microcrystalline planar size<sup>21</sup>  $L_a$ :

$$L_a = 44[I(D)/I(G)]^{-1} \quad (3)$$

where  $I(D)$  and  $I(G)$  are the integrated intensities of the D and G band, respectively.

The variation of the  $L_a$  decreased slightly with temperature up to  $1000^\circ\text{C}$  and then increased, as shown in Figure 5. The  $L_a$  values decreased from  $1.86$  to  $1.30\text{ nm}$  when the temperature rose from  $600$  to  $1000^\circ\text{C}$ . Above  $1000^\circ\text{C}$  the  $L_a$  values increased from  $1.30$  to  $2.61\text{ nm}$  at a heat-treatment temperature of  $2400^\circ\text{C}$ . As compared with the  $L_a$ , the  $L_c$  also grew very slowly in the temperature range of  $600$ – $1000^\circ\text{C}$ . This indicated the graphite layer planes grew along the  $c$  axis to from a crystal during this temperature range. These structures were also small and random, which were the isotropic structures. Above  $1000^\circ\text{C}$  the crystal grew along the in-plane directions, as well as the axis. However, the characteristic random configuration was maintained.

The relationship between the D band and G band intensities should be proportional to the degree of structural order ( $R$ ) with respect to the graphite structure, as shown below<sup>28</sup>:

$$R = I(D)/I(G) \quad (4)$$

The  $R$  value showed a slight increase in this ratio up to  $700^\circ\text{C}$  and gradual increased from  $700$  to  $1000^\circ\text{C}$ , as shown in Figure 7. The first increase of the intensity ratio at  $600$ – $700^\circ\text{C}$  seemed to indicate enhanced conversion of the organic polymer structure into a carbon macrostructure to form a glassy carbon. The formation of a glassy carbon was continuous with a temperature range of  $700$ – $1000^\circ\text{C}$ .

The increase of the  $R$  value indicated that the formation of glassy carbon was very random. These structures were amorphous contributions. Above  $1000^\circ\text{C}$  the crystalline structure was lengthened and broadened. Therefore, the  $L_c$  and

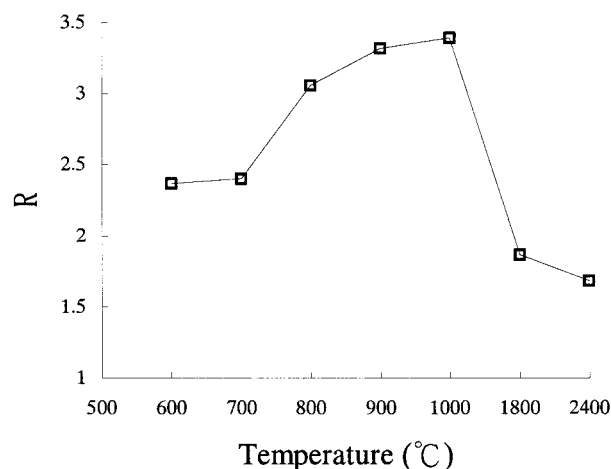


**Figure 7** The relationship between the degree of structural order ( $R$ ) of resulting carbonized resins and the pyrolysis temperature.

$L_a$  increased with an increase in the heat treatment (Fig. 5). This rearrangement of the crystalline structure led to a decrease in the D mode and an increase in the G mode. Therefore, this led to a decrease in the  $R$  value. However, the  $R$  value was higher than 1.5 at the heat-treatment temperature of 2500°C. This indicated that the graphitized resin was still a disordered material.

## CONCLUSIONS

The weight loss of the cured phenolic resin was significant between 400 and 700°C. Below 700°C the shrinkage also increased linearly with increasing temperature. The crystal size of the cured phenolic resins decreased with an increase in temperature. The crystal size decreased from 1.00 to 0.68 nm when the heat-treatment temperature rose from 230 to 500°C. Below 1000°C the  $L_c$  of the carbonized resin increased very little. Above 1000°C the stack size showed an increase with the increasing heat-treatment temperature. In the Raman spectra analysis the frequency of the G band for all carbonized and graphitized samples shifted to 1600  $\text{cm}^{-1}$  from 1582  $\text{cm}^{-1}$  for graphite. The D band shifted to 1330  $\text{cm}^{-1}$  from the 1357  $\text{cm}^{-1}$  value for imperfect carbon. This study indicated that the carbon layer planes grew along the  $c$  axis to from a crystal below 1000°C.

Above 1000°C the crystal grew along in-plane directions and the  $c$  axis. However, even when heat treated up to 2400°C, the graphitized resins consisted of a random configuration of small crystallites with stacks of several layers.

## REFERENCES

1. Grayson, M. Encyclopedia of Composite Materials and Components; Wiley: New York, 1983; p 10.
2. Fitzer, E. Carbon 1987, 25, 163.
3. Fitzer, E.; Huettner, W.; Manocha, L. M. Carbon 1980, 18, 291.
4. Savage, G. Carbon-Carbon Composites; Chapman & Hall: New York, 1993; Chap. 9.
5. Mckee, D. W. Carbon 1987, 24, 551.
6. Fitzer, E.; Gadow, R. Am Ceram Soc Bull 1986, 65, 326.
7. Fitzer, E.; Terwiwsch, B. Carbon 1972, 10, 383.
8. Yamashita, Y.; Ouchi, K. Carbon 1981, 19, 89.
9. Lausevic, Z.; Marinkovic, S. Carbon 1986, 24, 575.
10. Trick, K. A.; Saliba, T. E. Carbon 1995, 33, 1509.
11. Choe, C. R.; Lee, K. H.; Yoon, B. I. Carbon 1992, 30, 247.
12. Dillon, F.; Thomas, K. M.; Marsh, H. Carbon 1993, 31, 1337.
13. Ouchi, K. Carbon 1996, 4, 59.
14. Lum, R.; Wilkins, W.; Robbins, M.; Lyons, A. M.; Jones, R. P. Carbon 1983, 21, 111.
15. Ouchi, K.; Honda, H. Fuel 1959, 38, 429.
16. Ko, T. H.; Jaw, J. J.; Chein, Y. C. Polym Compos 1995, 16, 522.
17. Ko, T. H.; Ma, T. S. Polym Compos 1998, 19, 456.
18. Markovic, V.; Marinkovic, S. Carbon 1980, 18, 329.
19. Ko, T. H. Polym Sci 1991, 42, 1949.
20. Ko, T. H. J Appl Polym Sci 1991, 42, 1949.
21. Tuinstra, F.; Koenig, J. L. J Chem Phys 1970, 53, 1126.
22. Vidano, R.; Fischbach, D. B. J Am Ceram Soc 1978, 61, 13.
23. Beny-Bassez, C.; Rouzaud, J. N. Scan Electr Microsc 1985, 1, 119.
24. Rouzaud, J. N.; Oberlin, A.; Beny-Bassez, C. C R Acad Sci Paris Ser II 1983, 296, 369.
25. Cottinet, D.; Couderc, P.; Saint-Romain, J. L.; Dhamelincount, P. Carbon 1988, 26, 339.
26. Green, P. D.; Johnson, C. A.; Thomas, K. M. Fuel 1983, 62, 1013.
27. Cuesta, A.; Dhamelincount, P.; Laureyns, J.; Martinez-Alouso, A.; Tascon, J. M. D. Carbon 1994, 32, 1523.
28. Lespade, P.; Marchand, A.; Couzi, M.; Cruege, F. Carbon 1984, 22, 375.